

THE OFFICIAL MAGAZINE OF THE OCEANOGRAPHY SOCIETY

Oceanography

CITATION

Jan, S., C.-C. Chen, Y.-L. Tsai, Y.J. Yang, J. Wang, C.-S. Chern, G. Gawarkiewicz, R.-C. Lien, L. Centurioni, and J.-Y. Kuo. 2011. Mean structure and variability of the cold dome northeast of Taiwan. *Oceanography* 24(4):100–109, <http://dx.doi.org/10.5670/oceanog.2011.98>.

DOI

<http://dx.doi.org/10.5670/oceanog.2011.98>

COPYRIGHT

This article has been published in *Oceanography*, Volume 24, Number 4, a quarterly journal of The Oceanography Society. Copyright 2011 by The Oceanography Society. All rights reserved.

USAGE

Permission is granted to copy this article for use in teaching and research. Republication, systematic reproduction, or collective redistribution of any portion of this article by photocopy machine, reposting, or other means is permitted only with the approval of The Oceanography Society. Send all correspondence to: info@tos.org or The Oceanography Society, PO Box 1931, Rockville, MD 20849-1931, USA.

Mean Structure and Variability of the Cold Dome Northeast of Taiwan

BY SEN JAN, CHUNG-CHI CHEN, YA-LING TSAI, YIING JIANG YANG,
JOE WANG, CHING-SHENG CHERN, GLEN GAWARKIEWICZ,
REN-CHIEH LIEN, LUCA CENTURIONI, AND JIA-YU KUO



Deployment of a bottom-mounted acoustic Doppler current profiler on board R/V *Ocean Researcher 1* in Taiwanese waters during winter.
Photo courtesy of Sen Jan

ABSTRACT. The “cold dome” off northeastern Taiwan is one of the distinctive oceanic features in the seas surrounding Taiwan. The cold dome is important because persistent upwelling makes the region highly biologically productive. This article uses historical data, recent observations, and satellite-observed sea surface temperatures (SST) to describe the mean structure and variability of the cold dome. The long-term mean position of the cold dome, using the temperature at 50 m depth as a reference, is centered at 25.625°N, 122.125°E. The cold dome has a diameter of approximately 100 km, and is maintained by cold (< 21°C) and salty (> 34.5) waters upwelled along the continental slope. The ocean currents around the cold dome, although weak, flow counterclockwise. The monsoon-driven winter intrusion of the Kuroshio current onto the East China Sea shelf intensifies the upwelling and carries more subsurface water up to the cold dome than during the summer monsoon season. On a shorter timescale, the cold dome’s properties can be significantly modified by the passage of typhoons, which creates favorable physical conditions for short-term Kuroshio intrusions in summer. The surface expression of the cold dome viewed from satellite SST images is often not domelike but instead is an irregular shape with numerous filaments, and thus may contribute substantially to shelf/slope exchange. As a result of persistent upwelling, typhoon passage, and monsoon forcing, higher chlorophyll *a* concentrations, and thus higher primary productivity, are frequently observed in the vicinity of the cold dome.

INTRODUCTION

Subduction of the Philippine Sea Plate beneath the Eurasia Plate on geologic timescales created the island of Taiwan, Ryukyu Trench, Yaeyama Ridge, Ryukyu Island Arc, and Okinawa Trough (Figure 1a). The seafloor topography off northeastern Taiwan reflects this subduction regime, and includes a shallow continental shelf, a steep continental slope, a deep trench, and a steep rise with a series of submarine canyons (the Keelung Valley, the Mien-Hua Canyon, and the North Mien-Hua Canyon) that incise the continental shelf break (Figure 1a). The marine environment off northeastern Taiwan is as complex as the varying topography beneath it. To improve our understanding of the physical and associated biogeochemical processes in this region, the National Science Council

(NSC) of Taiwan sponsored an integrated observation program, Kuroshio Edge Exchange Processes (KEEP), from 1990 to 1994. The observational data obtained during KEEP revealed that the circulation over the complicated topography off northeastern Taiwan includes a persistent upwelling (named the “cold dome” by Chern and Wang [1990]), the Kuroshio, inflow from the Taiwan Strait current in summer and the China Coastal current in winter, strong tides, mesoscale eddies, internal waves, and atmospheric forcing such as monsoons and typhoons (tropical cyclones). Temporal and spatial variations of the cold dome will be described here using new measurements obtained from Taiwan-US collaborative experiments during 2008–2009 sponsored by the National Science Council under the project “Internal

wave and Typhoon-Ocean Interaction Project” (ITOP), and by the US Office of Naval Research under the program “Quantifying, Predicting, and Exploiting Uncertainty (QPE)” (Gawarkiewicz et al., 2011, in this issue). We also present seasonal observations of chlorophyll made at a station in the cold dome that suggest why the fisheries are so productive in this area.

Seasonal migration of the Kuroshio significantly modifies the flow pattern and associated hydrography in this region. The climatological mean of the historical shipboard acoustic Doppler current profiler (ADCP) and drifter trajectory data presented in Rudnick et al. (2011, in this issue) show that, off northeastern Taiwan, the Kuroshio turns northeastward along the continental shelf break in summer. During winter, the strong northeast monsoon opposes the Kuroshio (Chao, 1991), and a portion of the Kuroshio flows onto the continental shelf. Chao (1991), Chuang and Liang (1994), Tang et al. (2000), and Wu et al. (2008) studied the dynamics of these Kuroshio flows onto the continental shelf using in situ data or numerical simulations. Similar topographically induced intrusions and associated upwellings have been observed in the Gulf Stream system on the southeast US continental shelf (Atkinson, 1977; Blanton et al., 1981) and on the Charleston Bump off Charleston, South Carolina (Brooks and Bane, 1978). In the Gulf Stream, cold cyclonic eddies frequently carry cold water onto the continental shelf by interleaving or forming a bottom intrusion onto the shelf mostly during summer when the

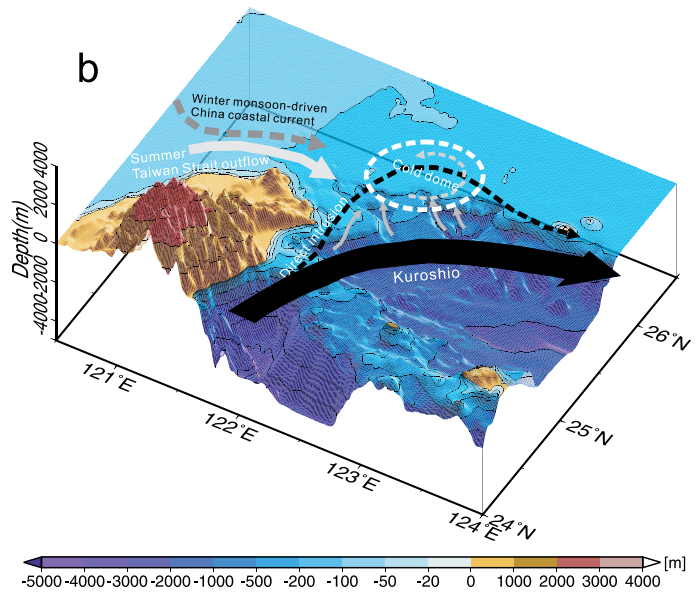
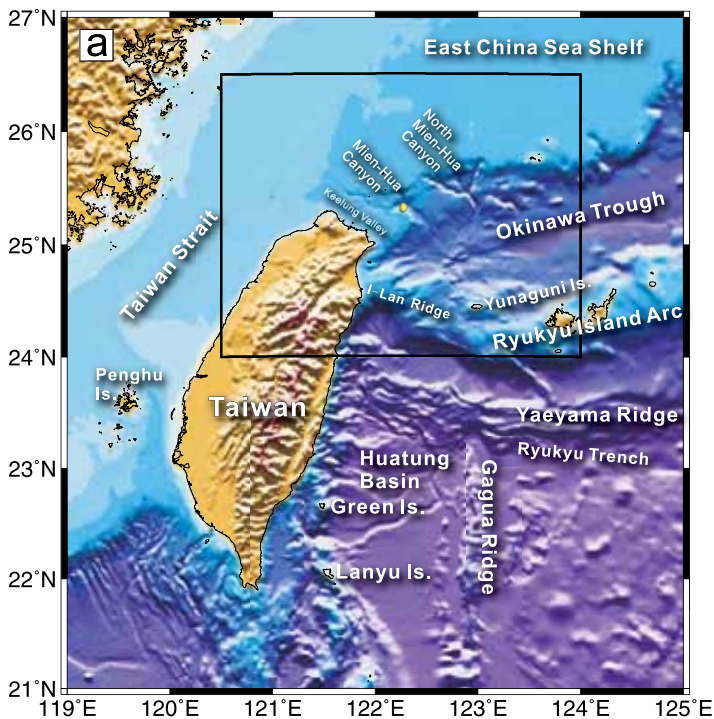


Figure 1. (a) Bathymetric chart for the seas around Taiwan. (b) Three-dimensional perspective view of the topography, the location of the cold dome, and the seasonal variation of the current pattern in the area bounded by the rectangle in (a).

shelf water mass is least dense (Atkinson, 1977; Blanton et al., 1981).

Different current systems carrying different water masses into this region modify the properties of the water masses off northeastern Taiwan, particularly in the upper 50 m of the ocean. At the seasonal timescale, the exchange of summer southwesterly and winter northeasterly monsoons dominate water mass

change (Jan et al., 2006). In summer, the Kuroshio remains offshore of the continental shelf, and the warm, relatively fresh Taiwan Strait water occupies the upper layer off northern Taiwan. In winter, the northeasterly monsoon carries cold and brackish China Coastal Water to the southern East China Sea, where it meets the water mass originating from the Kuroshio winter intrusions onto

the continental shelf. In summer and fall, the occasional passage of a typhoon across Taiwan leads to cold and saltier Kuroshio subsurface water upwelling onto the southern East China Sea shelf, where it lingers for a few days to weeks (e.g., Chern et al., 1990; Tang et al., 1999).

In addition to studies of the Kuroshio's variability and water mass exchange in the sea northeast of Taiwan, the cold dome, schematically shown in Figure 1b, has also been widely investigated over the past two decades not only because of its high productivity. The cold dome off northeastern Taiwan was originally named for its domelike hydrographic structure and counterclockwise circulation pattern (Chern and Wang, 1990; Tang et al., 2000). Cold dome water is supplied mostly by the ambient water mass over the continental slope, which is subsurface Kuroshio water mixed with shelf water, presumably by internal tide-enhanced vertical

Sen Jan (*senjan@ntu.edu.tw*) is Associate Professor, Institute of Oceanography, National Taiwan University, Taipei, Taiwan. **Chung-Chi Chen** is Professor, Department of Life Science, National Taiwan Normal University, Taipei, Taiwan. **Ya-Ling Tsai** is Postdoctoral Fellow, Institute of Oceanography, National Taiwan University, Taipei, Taiwan. **Yiing Jiang Yang** is Professor, Department of Oceanography, Chinese Naval Academy, Kaohsiung, Taiwan. **Joe Wang** is Professor, Institute of Oceanography, National Taiwan University, Taipei, Taiwan. **Ching-Sheng Chern** is Professor, Institute of Oceanography, National Taiwan University, Taipei, Taiwan. **Glen Gawarkiewicz** is Senior Scientist, Woods Hole Oceanographic Institution, Woods Hole, MA, USA. **Ren-Chieh Lien** is Principal Oceanographer and Affiliate Professor, Applied Physics Laboratory, University of Washington, Seattle, WA, USA. **Luca Centurioni** is Associate Project Scientist, Scripps Institution of Oceanography, La Jolla, CA, USA. **Jia-Yu Kuo** is Technician, Institute of Oceanography, National Taiwan University, Taipei, Taiwan.

mixing (Chern and Wang, 1990; Liu et al., 1992). During winter, the cold dome is either not present or is masked by frequent Kuroshio intrusions onto the continental shelf.

It is challenging to study the cold dome off northeastern Taiwan, particularly with moored instruments, because of the intense fishing activity in summer and high sea state in winter. Thus, gaps remain in our understanding of the formation process and the temporal and spatial variations of the cold dome. In this paper, we first present the general properties of the cold dome from a climatological viewpoint gained from years of at-sea data collection. We use satellite sea surface temperature (SST) observations to demonstrate that the shape of the cold dome is highly variable. We also present the associated biological response resulting from upwelling and summarize the physical processes responsible for cold dome changes on half-day to seasonal timescales.

CLIMATOLOGICAL MEAN OF THE COLD DOME

Temperature, salinity, and current velocity in the seas surrounding Taiwan have been measured from R/V *Ocean Researcher 1* since 1985, and R/Vs *Ocean Researcher 2* and 3 since 1994. The NSC Ocean Data Bank operated by National Taiwan University's Institute of Oceanography archives more than 40,000 conductivity-temperature-depth (CTD) casts (1985–2010) and 3,500,000 ADCP measurements from 16 m to 300 m depth (1991–2010). The raw data were quality controlled based on the standard procedure recommended by the US National Oceanic and Atmospheric Administration (NOAA) National Ocean Data Center.

A $0.25^\circ \times 0.25^\circ$ grid was chosen to be the horizontal resolution for the analysis of long-term statistics from the historical archives. The barotropic tidal current velocities computed from a two-dimensional regional tidal model (Hu et al., 2010) are subtracted from the raw ADCP data. Then, both the quality-assured CTD and de-tided ADCP data are interpolated to the center of each $0.25^\circ \times 0.25^\circ$ grid when there are more than three CTD data points and 30 ADCP data points in each grid.

Seasonal variations are primarily defined by the monsoon system in the region. The wind is predominantly northeasterly during the winter monsoon and southwesterly during the summer monsoon over the southern East China Sea and the northern South China Sea. The winter monsoon generally occurs from October to March and the summer monsoon from May to August. April and September are considered the monsoonal transition periods. Figure 2a and 2b depict

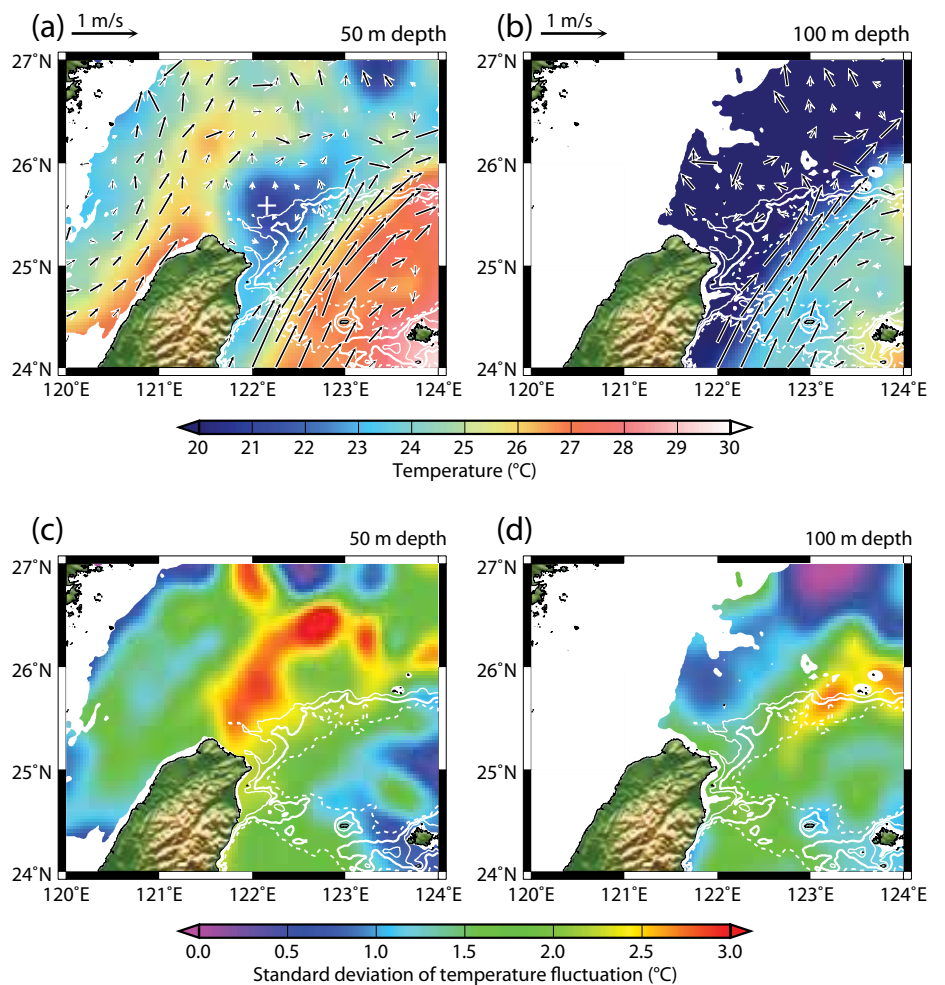


Figure 2. Climatological mean temperature and current velocity (black arrows) in summer (May–September) at depths of (a) 50 m and (b) 100 m and the corresponding standard deviation of temperature estimated from historical conductivity-temperature-depth (CTD) data at depths of (c) 50 m and (d) 100 m in each grid. The 200 m (thin white line), 500 m (thick white line), and 1,000 m (dashed white line) isobaths are plotted in each figure. The white + symbol in (a) marks the center of the cold dome.

the climatological mean summer temperature and the current velocity at 50 and 100 m depths, respectively. A disk-shaped cold water intrusion, with temperature about 21°C centered at 25.625°N, 122.125°E (white “+” in Figure 2a), is clearly seen off northeastern Taiwan between the warmer Kuroshio to the east and the cooler Taiwan Strait water to the west (Figure 2a). The cold dome’s diameter is approximately 100 km. The associated currents at 50 m depth, although weak, flow cyclonically (counterclockwise) around the cold dome, favoring upwelling in the cold dome’s center. Figure 2b indicates that the mean temperature at 100 m is less than 21°C over the continental shelf and to the left of the Kuroshio axis, and is greater than 23°C to the right of the Kuroshio. Horizontally, there is no cold-water source to supply the cold dome in the upper 100 m of the water column, so subsurface waters below 100 m must supply the 21°C water in the cold dome. In addition to the upwelling induced by the counterclockwise circulation, other mechanisms may be responsible for upwelling in the cold dome. For example, because the Kuroshio makes a right turn approximately following the curvature of the isobaths off northeastern Taiwan, a shoreward force, similar to the centrifugal force that arises in connection with rotation, drives the subsurface water shoreward (Shen et al., 2011). The shoreward flow favors upwelling along the continental slope of the southern East China Sea.

The magnitude of the temperature fluctuations can be evaluated from the standard deviation estimated from the historical CTD data in each grid. Figure 2c,d shows the standard

deviation of the temperature fluctuation at 50 m and 100 m depths, respectively. The standard deviation is less than 2°C in most regions at 50 m depth except in the cold dome region where the standard deviation reaches 2.5°C (Figure 2c), which suggests that the temperature in the cold dome varies significantly in summer. At 100 m depth, the standard deviation is a local minimum, < 1°C, compared to that surrounding the cold dome (Figure 2d), which further suggests that the cold dome is supplied by cold waters from 100 m depth and below.

RECENT OBSERVATIONS OF THE COLD DOME

A large-scale hydrographic survey was conducted from R/Vs *Ocean Researcher 2* and 3 during August 13–17, 2009. The observations were recorded one week after Typhoon Morakot, which brought record-breaking rainfall to, and wrought catastrophic damage in, southern Taiwan. The survey was part of a larger effort to quantify the uncertainty of regional ocean models in this area (Gawarkiewicz et al., 2011, in this issue). The well-organized campaign captured not only the freshwater pulse originating mostly from runoff due to Typhoon Morakot but also the cold dome’s three-dimensional hydrographic structure.

Figure 3 illustrates temperature and salinity distributions at 10 m and 100 m depths and at 25.5°N (line Z in Figure 3a) and 122.5°E (line M in Figure 3a) sections. Aside from a remarkable freshwater pulse with salinity below 32.5 off northern Taiwan (Figure 3c), a patch of northwest-southeast extending low-temperature (< 22°C) and high-salinity (> 34.3) water is found in the 10 m layer in Figure 3a

and 3c. From the zonal and meridional vertical hydrographic transects, doming of cold, saline water in the upper 150 m is evident from 122.2°E to 123°E in Figure 3e and 3f and from 25°N to 25.7°N in Figure 3g and 3h. Figure 3e–h suggests that the cold water upwelled from 200 m depth where the temperature was 16°C and the salinity 34.5.

The upwelling maintaining the cold dome could have been intensified by passage of Typhoon Morakot, which, in turn, may have caused the remarkable surface temperature decrease off northeastern Taiwan. Tsai et al. (2008) and Morimoto et al. (2009) discussed the processes responsible for this phenomenon based on modeling studies and observations of typhoons on a similar track. Typhoon-related processes affecting upwelling onto the shelf, and the associated biological impact, are discussed in a later section.

VARIABILITY OF THE COLD DOME STRUCTURE FROM SST PATTERNS

In comparison with the climatological mean shape of the cold dome, an instantaneous look at the cold patch on the sea surface does not often support that it is a “dome” exhibiting a circular pattern at the surface. To view the surface temperature signals of the cold dome, we downloaded and analyzed the multiple-satellite blended SST data from NOAA’s “Ocean Watch” web page (<http://las.pfeg.noaa.gov/oceanWatch/oceanwatch.php>). Taking into consideration blocking of the infrared remote-sensing signal of the daily SST due to cloud cover, eight-day composite 0.1° × 0.1° horizontal resolution SST data were used for the analysis. The eight-day composite SST filters out SST

variability shorter than eight days; even so, the shape of the cold water evident at the surface associated with the cold dome still varies greatly in time. The SST data in Figure 4 show the surface cold patch exhibiting different shapes at different times. Figure 4a shows that, in August 2008, the cold patch extended northward from the head of Mien-Hua Canyon to 26.5°N. In Figure 4b, the cold patch extends from the northern coast of Taiwan to North Mien-Hua Canyon along the continental shelf break in August 2009. Figure 4c shows the distribution of the cold patch looking more circular between Mien-Hua and North Mien-Hua Canyons in August 2010. Figure 4d indicates that, in September 2010, the cold patch shrank to a small area over Mien-Hua Canyon. Sometimes, the cold patch disappears in the SST data, particularly in winter, because the massive Kuroshio intrusion comprises the surface water overlying the cold dome while strong atmospheric cooling at the sea surface reduces the temperature contrast in the horizontal.

The surface appearance and the associated upwelling strength of the cold dome can be inferred from the SST difference between the cold dome's mean location (25.25°–25.75°N, 122°–122.5°E; box A in Figure 4a) and a particular region southeast of the cold dome, that is, in the Kuroshio (24.5–25°N, 122.5–123°E; box B in Figure 4a). Higher contrast between the SST of the cold dome (the cold patch at the surface) and its surrounding area is associated with stronger upwelling in the cold dome. Figure 4e shows the multiple-satellite blended daily SSTs averaged over the two regions and their difference during January 2006 and May 2010. SST seasonal values range

from 20°C to 30°C in the cold dome and from 23°C to 30.5°C in the Kuroshio region in this period. In addition to the seasonality, there is significant intra-seasonal (from periods longer than a day to shorter than seasonal timescale) SST variation (> 2°C) in both regions.

Some of the SST decreases were related to complicated oceanic responses to typhoons, for example, Typhoons Sepat in mid-August 2007, Fung-Wong in late July 2008, Sinlaku in mid-September 2008, and Morakot in early August 2009. The seasonality of the SST difference

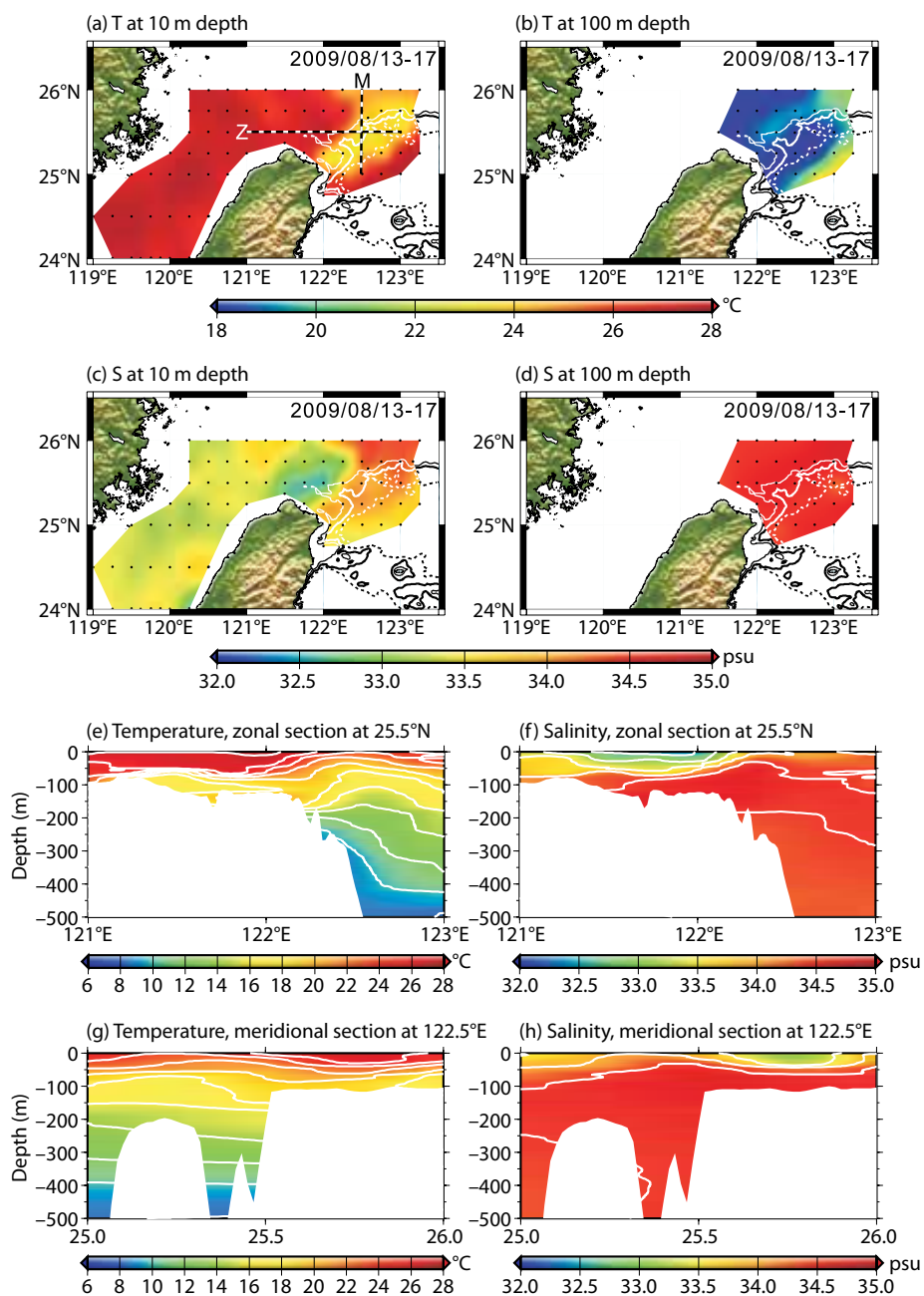


Figure 3. Temperature and salinity distribution at 10 m and 100 m (a–d), at a 25.5°N zonal section (e and f; line Z in a), and at a 122.5°E meridional section (g and h; line M in a) during August 13–17, 2009. Dots indicate CTD stations. Isobaths in a–d are the same as those in Figure 2.

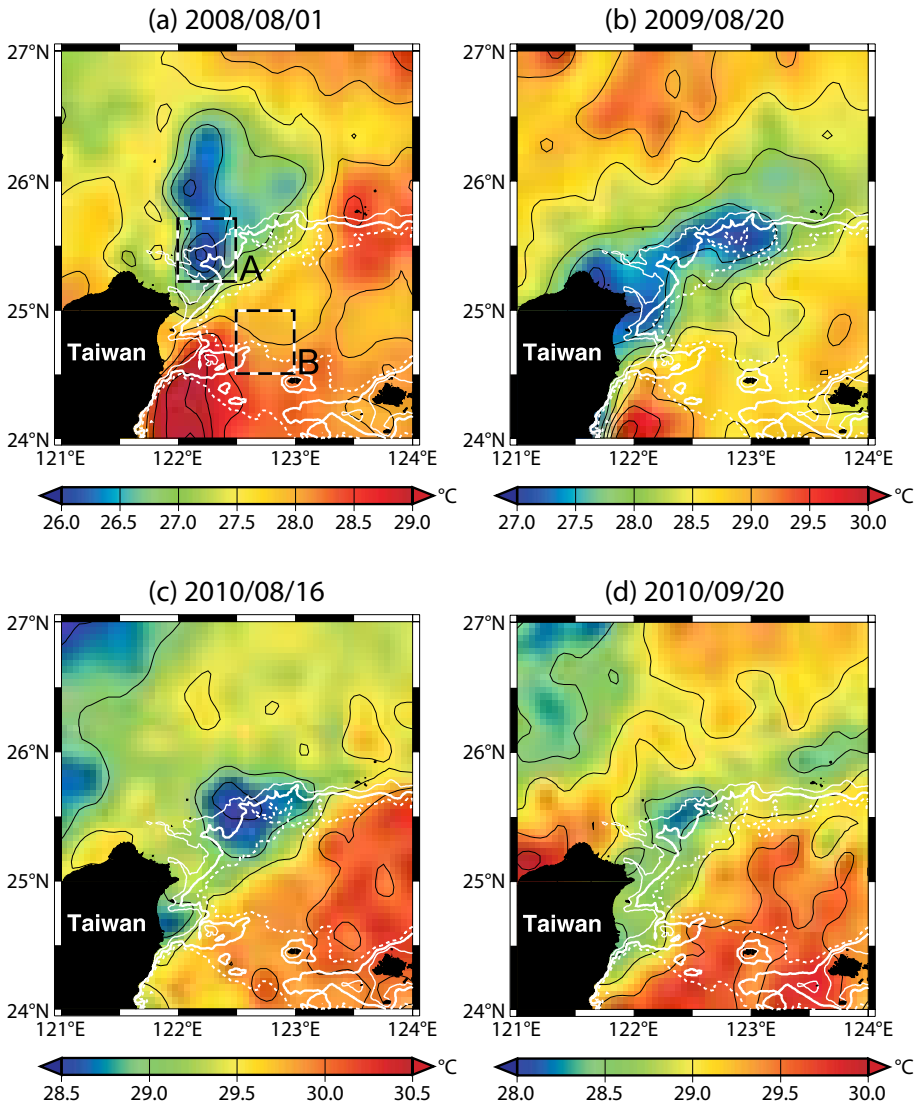


Figure 4. Multiple-satellite blended, eight-day composite sea surface temperature (SST) centered on (a) August 1, 2008, (b) August 20, 2009, (c) August 16, 2010, and (d) September 6, 2010. (e) Time series of daily SST averaged over the climatological mean location of the cold dome (blue line; box A in 4a) and the Kuroshio region (red line; box B in 4a), and the SST difference between the two regions. Arrows in (e) mark the passages of Typhoons Sepat, Fung-Wong, Sinlaku, and Morakot. Isobaths in a–d are the same as those in Figure 2.

between the two regions in Figure 4e, although not clear, indicates that the SST difference is relatively small ($< 2^{\circ}\text{C}$) in summer (July–September) and increases to $> 3^{\circ}\text{C}$ mostly in spring (February–April) and fall (October–November).

Intense solar heating and heat advection by ocean currents in summer lead to smaller spatial contrast in SST during that season than in spring and fall, presumably leading to a smaller probability that the surface cold patch will appear. However, when favorable processes in summer strengthen upwelling, for example, after typhoons, spatial contrast of SST increases. In winter, intrusion of the Kuroshio into the East China Sea and large-scale atmospheric cooling also reduce the SST contrast between the two regions. The frequency of the cold dome evident in SST is higher in spring and fall compared to summer and winter.

BIOLOGICAL ASPECTS OF THE COLD DOME

To gain a basic understanding of the biological aspects of the cold dome and its variability, we provide some of the results from the Long-term Observation and Research of the East China Sea (LORECS) program sponsored by NSC. The sampling station (25.42°N , 122.21°E) was located close to the center of the cold dome (yellow dot in Figure 1a), where the water depth is 250 m. Samples were collected from R/V *Ocean Researcher 2* during the period January 2004 to January 2005, at sampling intervals of one to three months. The seawater was sampled at six water depths—5, 10, 20, 50, 75, and 100 m—using 10-liter Teflon-coated Go-Flo bottles mounted on a General Oceanic rosette assembly. Hydrographic data were collected using

a CTD down to 200 m depth. Chen et al. (2009) detail the analytic methods used to determine chlorophyll *a* and inorganic nutrients (e.g., nitrate).

The depth at which temperature is $< 21^{\circ}\text{C}$ and salinity > 34.5 is used as the reference depth for upwelled subsurface water. In winter, this combination of temperature and salinity does not provide a good estimate of the vertical displacement of upwelling because the upper layer's temperature and salinity are also around 21°C and 34.5, respectively, off northeastern Taiwan due to the Kuroshio intrusion. Regardless of this concern, Figure 5 shows that the upwelled water reached closer to the surface during the winter northeast monsoon than during the summer southwest monsoon. The subsurface water upwelled to a depth of 3 to 61 m throughout the year. For comparison, a reference depth of 163.0 ± 15.8 m (mean \pm SD) was measured in the same observational period at a nearby station (25.08°N , 123.15°E) outside the cold dome. It was anticipated that the upwelled waters of the cold dome would have higher nutrient concentrations than the surrounding waters, and that the measured nutrient concentrations would be related to the strength of the event. Indeed, the data show that the average nitrate concentration sampled at 100 m depth in the cold dome is higher during the winter northeast monsoon than during the summer southwest monsoon (Figure 5). An exception is the anomalously high nitrate concentration measured on April 5, 2004, (Figure 5) that may have been caused by a passing Asian dust storm (Hung et al., 2009).

It is interesting to note that during the study period, higher phytoplankton biomass was measured in summer than

in the high nutrient-enriched period of the winter monsoon (Figure 5). This unexpected relationship could be attributed to atmospheric input (e.g., the Asian dust storm), different sources of water to this region, or dilution (subsurface water with lower phytoplankton biomass upwelled to the surface layer). This issue deserves further study.

DYNAMICS OF COLD DOME FLUCTUATION

The Kuroshio, Taiwan Strait, and China coastal currents, as well as the monsoons, affect the size and shape of the cold dome. Swift tidal currents, internal tides/waves, typhoons, and mesoscale eddies also affect the cold dome. The seasonal effect of the Kuroshio intrusion has been widely studied (e.g., see Chern et al., 1990; Chao, 1991; Hsueh et al., 1992; Chern and Wang, 1992; Tang et al., 1999, 2000; Wu et al., 2008).

On the intraseasonal timescale, mesoscale eddies affect the Kuroshio, especially the volume transport between Yunaguni Island and Taiwan (i.e., the World Ocean Circulation Experiment PCM-1 transect). Johns et al. (2001) found that when a clockwise eddy reached the Kuroshio east of Taiwan, the northward current and associated transport of the Kuroshio increased. Consequently, the Kuroshio can climb up to the shelf and enhance the upwelling that supplies the cold dome. A counterclockwise eddy, on the other hand, does not favor Kuroshio intrusion.

Swift barotropic tidal currents off the northern coast of Taiwan periodically drive the cold dome westward and eastward approximately two times a day (the semidiurnal tide). The horizontal excursion of the cold dome reaches ~ 20 km, estimated using a mean velocity amplitude of the semidiurnal tidal current, 1 m s^{-1} (Jan et al., 2004), and the

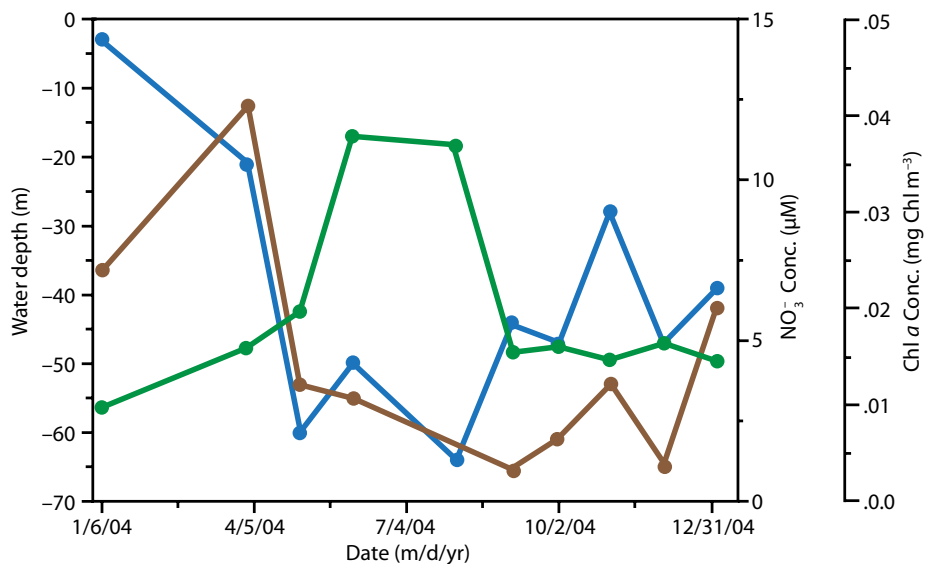


Figure 5. Temporal variations of water depth where water temperature $< 21^{\circ}\text{C}$ and salinity > 34.5 (blue), averaged nitrate (NO_3^-) concentration over 100 m of water column (brown), and averaged chlorophyll *a* concentration over 100 m of water column (green). The given water depth can be interpreted as the uppermost depth to which subsurface water reaches.

duration of a half-period of the semidiurnal tide, 6 h. In addition to horizontal movement, internal tides excited at the continental slope push cold dome water up and down at tidal frequencies. Results of an anchored CTD measurement obtained in August 2008 show that the vertical displacement of the isotherms reached 40 m in the cold dome region. This observation suggests that the cold

significant surface cooling in the traditional cold dome region after the passage of Typhoon Haitang (2005) using multiple-satellite remote-sensing data. Morimoto et al. (2009) also observed this event using an ocean radar system mounted on Yonaguni and Ishigaki islands. The impact of Typhoon Morakot on the cold dome is likely similar to the impact of these events.

slope to the cold dome on the shelf edge. Accompanying the physical process, the biogeochemical parameters are considerably changed, and production increases through complicated biological processes in the cold dome area (Hung et al., 2010; Hung and Gong, 2011, in this issue).

SUMMARY

Analysis of a compilation of historical CTD, ADCP, and composite satellite SST data and recent measurements improves our understanding of the cold dome and its energetic variability off northeastern Taiwan. The center of the cold dome is 25.625°N, 122.125°E, and it has a diameter of approximately 100 km and a weak counterclockwise circulation around it, particularly in summer. Upwelling supplies cold (< 21°C) and saltier (> 34.5) subsurface waters to the cold dome from greater than 100 m depth. Generally, the cold dome is more easily identified at the sea surface in summer than in winter because the massive winter intrusion of the Kuroshio overlies the cold dome and thus reduces its surface expression.

Joint observations from ITOP and QPE further reveal that the cold dome varies at shorter temporal and spatial scales as a result of complicated oceanic and atmospheric forcings. In contrast to the climatology of the cold dome, multiple-satellite SST images suggest that the cold dome's shape at the surface is often irregular and filamentary. In addition to the influence of seasonal Kuroshio intrusion, many processes affect the cold dome, for example, internal waves, typhoon winds, and ocean eddies. These processes are not well understood and will be explored further through programs such as ITOP and QPE.

“ THE ‘COLD DOME’ OFF NORTHEASTERN TAIWAN IS ONE OF THE DISTINCTIVE OCEANIC FEATURES IN THE SEAS SURROUNDING TAIWAN. ”

dome water mass may extend to the surface during the upward phase of an internal tide.

Short-duration Kuroshio intrusions in summer can also modify cold dome properties. Typhoon passages around this region were the primary causes of intrusions observed by several field surveys. Chern et al. (1990) conducted a post-storm hydrographical survey and measured an increase in cooling and salinity on the shelf and near the cold dome after Typhoon Gerald (1987) had passed through Taiwan Strait from the south. Chuang and Liang (1994) observed several summer intrusion events in the moored current meter data and identified corresponding typhoon passages around this region. Similarly, using shipboard CTD and ADCP measurements, Tang et al. (1999) observed a Kuroshio intrusion after Typhoon Doug (1994). More recently, Chang et al. (2008) demonstrated

According to Tsai et al. (2008) and Morimoto et al. (2009), the typhoon-induced Kuroshio intrusion can contribute to the enhancement of upwelling off northeastern Taiwan through two potential physical processes. The first process is the impediment of the northward Taiwan Strait outflow and the shoreward movement of the Kuroshio (i.e., the Ekman drift in the Northern Hemisphere) due to the northeasterly-northerly winds during the first half of the typhoon passage. The second process is the speeding up of the Kuroshio after it is forced toward the northeast coast of Taiwan due to the southwesterly-southerly winds during the second half of the typhoon passage. The first process weakens the blocking effect of the Taiwan Strait outflow to the Kuroshio and therefore favors Kuroshio intrusion. The subsequent process enhances the upwelling that supplies the cold subsurface water along the continental

ACKNOWLEDGEMENTS

The National Science Council (NSC) of Taiwan sponsored this study under grant NSC98-2611-M-002-019-MY3. NSC supported C.-C. Chen under grant NSC98-2611-M-003-001-MY3. The NSC Ocean Data Bank provided historical CTD and ADCP data and 500 m resolution East Asian Seas bathymetric data in accordance with the Data Release Policy. Comments from Larry Atkinson and an anonymous reviewer substantially improved this paper. We acknowledge the US NOAA CoastWatch Program, NOAA NESDIS Office of Satellite Data Processing and Distribution, and the NASA Goddard Space Flight Center OceanColor Web. 

REFERENCES

- Atkinson, L.P. 1977. Modes of Gulf Stream intrusion into the South Atlantic Bight shelf waters. *Geophysical Research Letters* 4(12):583–586, <http://dx.doi.org/10.1029/GL004i012p00583>.
- Blanton, J.O., L.P. Atkinson, L.J. Pietrafesa, and T.N. Lee. 1981. The intrusion of Gulf Stream water across the continental shelf due to topographically induced upwelling. *Deep-Sea Research* 28A(4):393–405.
- Brooks, D.A., and J.M. Bane Jr. 1978. Gulf Stream deflection by a bottom feature off Charleston, South Carolina. *Science* 201:1,225–1,226, <http://dx.doi.org/10.1126/science.201.4362.1225>.
- Chang, Y., H.-T. Liao, M.-A. Lee, J.-W. Chan, W.-J. Shieh, K.-T. Lee, G.-H. Wang, and Y.-C. Lan. 2008. Multisatellite observation on upwelling after the passage of Typhoon Hai-Tang in the southern East China Sea. *Geophysical Research Letters* 35, L03612, <http://dx.doi.org/10.1029/2007GL032858>.
- Chao, S.-Y. 1991. Circulation of the East China Sea: A numerical study. *Journal of the Oceanography Society of Japan* 46:273–295.
- Chen, C.-C., F.-K. Shiah, K.-P. Chiang, G.-C. Gong, and W.M. Kemp. 2009. Effects of the Changjiang (Yangtze) River discharge on planktonic community respiration in the East China Sea. *Journal of Geophysical Research* 114, C03005, <http://dx.doi.org/10.1029/2008JC004891>.
- Chern, C.-S., and J. Wang. 1990. On the mixing of waters at a northern offshore area of Taiwan. *Terrestrial Atmospheric and Oceanic Sciences* 1(3):297–306.
- Chern, C.-S., and J. Wang. 1992. The influence of Taiwan Strait waters on the circulation of the southern East China Sea. *La mer* 30:223–228.
- Chern, C.-S., J. Wang, and D.-P. Wang. 1990. The exchange of Kuroshio and East China Sea shelf water. *Journal of Geophysical Research* 95(C9):16,017–16,023.
- Chuang, W.-S., and W.-D. Liang. 1994. Seasonal variability of intrusion of the Kuroshio water across the continental shelf northeast of Taiwan. *Journal of Oceanography* 50:531–542, <http://dx.doi.org/10.1007/BF02235422>.
- Gawarkiewicz, G., S. Jan, P.F.J. Lermusiaux, J.L. McClean, L. Centurioni, K. Taylor, B. Cornuelle, T.F. Duda, J. Wang, Y.J. Yang, and others. 2011. Circulation and intrusions northeast of Taiwan: Chasing and predicting uncertainty in the cold dome. *Oceanography* 24(4):110–121, <http://dx.doi.org/10.5670/oceanog.2011.99>.
- Hsueh, Y., J. Wang, and C.-S. Chern. 1992. The intrusion of the Kuroshio across the continental shelf northeast of Taiwan. *Journal of Geophysical Research* 97(C9):14,323–14,330, <http://dx.doi.org/10.1029/92JC01401>.
- Hu, C.-K., C.-T. Chiu, S.-H. Chen, J.-Y. Kuo, S. Jan, and Y.-H. Tseng. 2010. Numerical simulation of barotropic tides around Taiwan. *Terrestrial Atmospheric and Oceanic Sciences* 21(1):71–84, [http://dx.doi.org/10.3319/TAO.2009.05.25.02\(IWNOP\)](http://dx.doi.org/10.3319/TAO.2009.05.25.02(IWNOP)).
- Hung, C.-C., G.-C. Gong, W.-C. Chung, W.-T. Kuo, and F.-C. Lin. 2009. Enhancement of particulate organic carbon export flux induced by atmospheric forcing in the subtropical oligotrophic northwest Pacific Ocean. *Marine Chemistry* 113:19–24, <http://dx.doi.org/10.1016/j.marchem.2008.11.004>.
- Hung, C.-C., G.-C. Gong, W.-C. Chou, C.-C. Chung, M.-A. Lee, Y. Chang, H.-Y. Chen, S.-J. Huang, Y. Yang, W.-R. Yang, and others. 2010. The effect of typhoon on particulate organic carbon flux in the southern East China Sea. *Biogeosciences* 7:3,007–3,018, <http://dx.doi.org/10.5194/bg-7-3007-2010>.
- Hung, C.-C., and G.-C. Gong. 2011. Biogeochemical responses in the southern East China Sea after typhoons. *Oceanography* 24(4):42–51, <http://dx.doi.org/10.5670/oceanog.2011.93>.
- Jan, S., C.-S. Chern, J. Wang, and S.-Y. Chao. 2004. The anomalous amplification of M_2 tide in the Taiwan Strait. *Geophysical Research Letters* 31, L07308, <http://dx.doi.org/10.1029/2003GL019373>.
- Jan, S., D.D. Sheu, and H.M. Kuo. 2006. Water mass and throughflow transport variability in the Taiwan Strait. *Journal of Geophysical Research* 111, C12012, <http://dx.doi.org/10.1029/2006JC003656>.
- Johns, W.E., T.N. Lee, D. Zhang, R. Zantopp, C.-T. Liu, and Y. Yang. 2001. The Kuroshio east of Taiwan: Moored transport observations from the WOCE PCM-1 array. *Journal of Physical Oceanography* 31:1,031–1,053, [http://dx.doi.org/10.1175/1520-0485\(2001\)031<1031:TKEOTM>2.0.CO;2](http://dx.doi.org/10.1175/1520-0485(2001)031<1031:TKEOTM>2.0.CO;2).
- Liu, K.K., G.-C. Gong, S. Lin, C.Y. Yang, C.L. Wei, S.-C. Pai, and C.-K. Wu. 1992. The year-round upwelling at the shelf break near the northern tip of Taiwan as evidenced by chemical hydrography. *Terrestrial Atmospheric and Oceanic Sciences* 3:243–275.
- Morimoto, A., S. Kojima, S. Jan, and D. Takahashi. 2009. Movement of the Kuroshio axis to the northeast shelf of Taiwan during typhoon events. *Estuarine, Coastal and Shelf Sciences* 82:547–552, <http://dx.doi.org/10.1016/j.jecss.2009.02.022>.
- Rudnick, D., S. Jan, L. Centurioni, C.M. Lee, R.-C. Lien, J. Wang, D.-K. Lee, R.-S. Tseng, Y.Y. Kim, and C.-S. Chern. 2011. Seasonal and mesoscale variability of the Kuroshio near its origin. *Oceanography* 24(4):52–63, <http://dx.doi.org/10.5670/oceanog.2011.95>.
- Shen, M.-L., Y.-H. Tseng, and S. Jan. 2011. The formation and dynamics of the cold-dome off northeastern Taiwan. *Journal of Marine Systems* 86:1–2, <http://dx.doi.org/10.1016/j.jmarsys.2011.01.002>.
- Tang, T.-Y., Y. Hsueh, Y.-J. Yang, and J.-C. Ma. 1999. Continental slope flow northeast of Taiwan. *Journal of Physical Oceanography* 29:1,353–1,362, [http://dx.doi.org/10.1175/1520-0485\(1999\)029<1353:CSFNOT>2.0.CO;2](http://dx.doi.org/10.1175/1520-0485(1999)029<1353:CSFNOT>2.0.CO;2).
- Tang, T.-Y., J.H. Tai, and Y.J. Yang. 2000. The flow pattern north of Taiwan and the migration of the Kuroshio. *Continental Shelf Research* 20:349–371, [http://dx.doi.org/10.1016/S0278-4343\(99\)00076-X](http://dx.doi.org/10.1016/S0278-4343(99)00076-X).
- Tsai, Y., C.-S. Chern, and J. Wang. 2008. Typhoon induced upper ocean cooling off northeastern Taiwan. *Geophysical Research Letters* 35, L14605, <http://dx.doi.org/10.1029/2008GL034368>.
- Wu, C.-R., H.-F. Lu, and S.-Y. Chao. 2008. A numerical study on the formation of upwelling off northeast Taiwan. *Journal of Geophysical Research* 113, C08025, <http://dx.doi.org/10.1029/2007JC004697>.